

# Notes

## Nonlinear Stability of Microscopic Polymer Films with Slippage

Ashutosh Sharma\* and Rajesh Khanna

Department of Chemical Engineering, Indian Institute of Technology at Kanpur, Kanpur 208016, India

Received April 24, 1996

Revised Manuscript Received May 2, 1996

The instability, breakup, and dewetting of thin (<100 nm) films on nonwetable surfaces are caused by the conjoining pressure engendered by the long-range (e.g., Lifshitz–van der Waals) interactions.<sup>1–3</sup> Most of the experimental studies<sup>4–8</sup> of thin-film stability employ polymeric liquids, which allow time-resolved experiments without significant mass loss. Thin polymer films are also used as coatings in a variety of settings.

In contrast to simple liquids, entangled polymer melts slip at smooth, inert surfaces which greatly modifies its wetting behavior.<sup>5,9,10</sup> The purpose of this short note is to extend the linear stability analysis<sup>10</sup> to the nonlinear regime and thus quantify the effects of slippage on the length and time scales of the thin-film stability leading to rupture. Some recent experiments<sup>4,6–8</sup> on the stability of thin polymer films are interpreted within the proposed framework.

Equations of continuity and motion in the thin film (small slope) approximation are<sup>1,2</sup>

$$u_x + v_z = 0 \quad (1)$$

$$p_z + \phi_z = 0 \quad (2)$$

$$\mu u_{zz} = p_x + \phi_x \quad (3)$$

where subscripts denote differentiation,  $x$  and  $z$  are coordinates parallel and normal to the solid surface, respectively,  $u$  and  $v$  are the  $x$  and  $z$  components of velocity,  $p$  is pressure,  $\mu$  is viscosity, and  $(-\phi)$  denotes excess body force (per unit volume) due to long-range interactions.

Boundary conditions at the solid surface ( $z = 0$ ) and the free surface of the film ( $z = h$ ) are

$$z = 0: v = 0 \text{ and } u_z = b^{-1}u \quad (4)$$

$$z = h(x, t): u_z = 0 \text{ and } p_x = -\gamma h_{xxx} \quad (5)$$

where  $\gamma$  is surface tension and  $b$  is a slip length discussed in detail elsewhere ( $b = \mu/\mu_s$ ;  $\mu_s$  is the friction coefficient).<sup>5,9,10</sup> For simple liquids,  $b$  is a molecular size ( $b \sim a$ ), so that the no-slip condition ( $u \rightarrow 0$ ) is recovered at the solid surface. Entangled polymer melts are extremely viscous,  $\mu \sim \mu_0(N^3/N_e^2)$ , where  $\mu_0$  ( $\sim 1$  cP) is a monomer viscosity,  $N$  is the polymerization index, and  $N_e$  ( $\sim 10^2$ ) is the threshold of entanglements.<sup>5,9,10</sup> Thus,  $b \sim a(\mu/\mu_0)$  can be of the order of tens of micrometers

for viscous ( $\mu \sim 100$  cP) melts. Large values of  $b$  ( $\gg h$ ) imply plug flow in the film.

Solutions of eqs 1–3, together with conditions (4) and (5), and the kinematic condition,  $h_t + uh_x = v$  at  $z = h$ , give an equation of evolution for the film thickness.

$$3\mu h_t + \gamma[h^2(h + 3b)h_{xxx}]_x - [h^2(h + 3b)\phi_x]_x = 0 \quad (6)$$

The potential due to Lifshitz–van der Waals (LW) forces on a nonwetable surface is<sup>11</sup>

$$\phi = \frac{A}{6\pi h^3} = -\frac{2Sd_0^2}{h^3}; \quad A > 0, S < 0 \quad (7)$$

where  $A$  is the effective Hamaker constant denoting the difference between liquid–liquid and liquid–solid Hamaker constants; i.e.,  $A = A_{LL} - A_{SL}$ .  $S = -A/12\pi d_0^2$  is the LW component of the spreading coefficient,<sup>11</sup> and  $d_0$  ( $\sim 0.158$  nm) is a cut-off separation distance<sup>3,11</sup> due to the Born repulsion. In the absence of short-range forces,  $S$  is also related to the macroscopic equilibrium contact angle  $\theta$  by the Young–Dupre equation,  $S = \gamma(1 - \cos \theta)$ . Equations 6 and 7 lead to

$$3\mu h_t + \left[ (h + 3b) \left\{ \gamma h^2 h_{xxx} - \left( \frac{6Sd_0^2}{h^2} \right) h_x \right\} \right]_x = 0 \quad (8)$$

Linearization around the mean film thickness,  $h_0$ , gives periodic solutions,  $h = h_0 + \varepsilon \exp(ikx + \omega t)$ . The initial growth rate ( $\omega$ ) of small-amplitude ( $\varepsilon$ ) disturbances with wavenumber  $k$  in the linear regime is

$$\omega = (h_0 + 3b)k^2[(-6Sd_0^2/h_0^2) - \gamma h_0^2 k^2]/3\mu \quad (9)$$

For partially wettable ( $S < 0$ ) surfaces, the film is unstable to disturbances with  $k < k_c = (-6S/\gamma)^{1/2}(d_0/h_0^2)$ . The fastest growing disturbance ( $\partial\omega/\partial k_m = 0$ ) in the linear regime evolves on a length scale  $\lambda_m = 2\pi/k_m$ , where

$$\lambda_m = 2\pi h_0 \left( \frac{h_0}{d_0} \right) \left( \frac{\gamma}{3|S|} \right)^{1/2} = 2\pi h_0 \left( \frac{h_0}{d_0} \right) [3(1 - \cos \theta)]^{-1/2} \quad (10)$$

If we extrapolate the linear theory all the way to the instant of rupture, an estimate of the breakup time is obtained as ( $t_L = \ln(h_0/\varepsilon)/\omega_m$ ):

$$t_L = \left[ 1 + \left( \frac{3b}{h_0} \right) \right]^{-1} \left[ \frac{\mu \gamma h_0^5}{3S^2 d_0^4} \ln \left( \frac{h_0}{\varepsilon} \right) \right] \quad (11)$$

The linear instability analysis with LW forces has been considered previously<sup>10</sup> in a slightly different form. The analysis can be easily extended to include the non-LW shorter range interactions.<sup>11</sup> However, there is a possibility that the nonlinearities in eq 8 can greatly modify the length and time scales, since the destabilizing term grows stronger as  $(h^{-2}h_x)_x$  at locally thin spots ( $h \rightarrow 0$ ). The effect of nonlinearities can be represented in the

\* To whom correspondence should be addressed. Fax: 91-512-250007 or 250260; Phone: 91-512-257026; e-mail: ashutos@iitk.ernet.in.

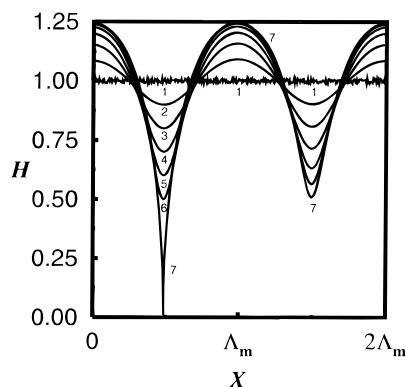


**Figure 1.** Evolution of the instability starting with a random small amplitude ( $\epsilon = 0.01$ ) disturbance (curve 1), in the case of strong slip ( $B \gg 1$ ,  $\tau = BT$ ). A coherent two-cell structure emerges in the simulation length chosen ( $0 \leq X \leq 2\Lambda_m$ ). Curves 2–7 refer to  $\tau = 20.96, 23.18, 24.12, 24.54, 24.72$ , and  $24.80$ , respectively.

most compact form by introducing in eq 8 the following nondimensional scales: A lone parameter ( $B = 3b/h_0$ )

$$H = h/h_0, X = (x/h_0)(6|S|d_0^2/\gamma h_0^2)^{1/2}, T = t(12S^2d_0^4/\mu\gamma h_0^5)$$

remains in the nondimensional version,

$$H_T + \left[ H^2(H+B) \left\{ H_{XX} - \left( \frac{1}{3} \right) H^3 \right\} \right]_{X|X} = 0 \quad (12)$$

From the linear theory, the nondimensional counterparts of eqs 10 and 11 are  $\Lambda_m = 2\sqrt{2}\pi$  and  $T_L = 4(1+B)^{-1} \ln \epsilon$ , where  $\epsilon = (h_0/\epsilon)$ . Under conditions of strong slip ( $B \gg H \sim O(1)$ ),  $B$  can also be removed by redefining the time scale as  $\tau = BT \sim O(1)$ . Equation 12 governs not only the film breakup but also growth of holes on the surface, and thus time scales for hole formation and dewetting are both greatly reduced by strong slippage. The length scale, however, remains unaltered.

Equation 12 was discretized with the help of successive central differencing with half-node interpolations, and the time integration was performed by the Gear method suitable for stiff equations. For  $0 \leq X \leq \Lambda_m$ , 200 grids were found to be adequate for grid convergence. We found that a small number of grids ( $< 50$ ), as in a pioneering work<sup>2</sup> on nonslipping ( $B = 0$ ) films, led to numerical errors.

In the case of strong slip ( $B \gg 1$ ), Figure 1 shows the evolution of instability in  $0 \leq X \leq 2\Lambda_m$ , starting with a small ( $\epsilon = 0.01$ ) random disturbance. The initial random disturbances are quickly reorganized on the length scale ( $\Lambda_m$ ) of the dominant linear wave, and further evolution continues on this scale until the film breakup. Note that the nondimensional  $X$  scale is greatly compressed. Dimensional length scale ( $\lambda_m$ ) of the instability is several orders of magnitude larger than the mean film thickness (eq 10), and slopes are indeed small. The film thickness away from the hole remains undisturbed during the strongly nonlinear, explosive phase of the instability ( $H_{\min} < 0.6$ ).

Figure 2 addresses the problem of nonlinear mode selection for different initial amplitudes. The variation of actual (nonlinear) breakup times,  $T_R$  or  $\tau_R$  (for  $B \gg 1$ ), with the wavelength ( $\Lambda$ ) and amplitude of disturbances are summarized in Figure 2. For conditions of no slip ( $B = 0$ ), moderate slip ( $B = 1$ ), and strong slip ( $B \gg 1$ ), the dominant nonlinear wave is only slightly

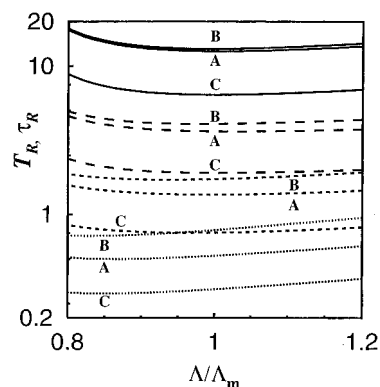


**Figure 2.** Variations of nonlinear breakup times ( $T_R$  or  $\tau_R$  for  $B \gg 1$ ) with the wavelength and amplitude of initial disturbances. Labels A, B, and C refer to the cases of  $B \gg 1$ ,  $B = 1$ , and  $B = 0$ , respectively.  $\epsilon = 0.01$  (—);  $\epsilon = 0.1$  (---);  $\epsilon = 0.2$  (- - -);  $\epsilon = 0.3$  (····). The minimum time of rupture occurs for  $\Lambda \approx \Lambda_m$ .

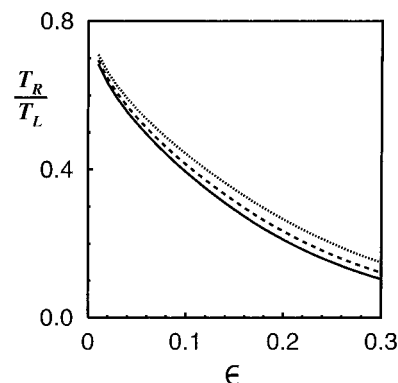


**Figure 3.** Ratio of breakup times from the nonlinear and linear analysis.  $B = 0$  (····);  $B = 1$  (---);  $B \gg 1$  (—).

smaller than  $\Lambda_m$ , implying that the wavelengths in the range,  $0.5\Lambda_m < \Lambda < 1.3\Lambda_m$ , can produce rupture on comparable time scales. This is one of the factors which can introduce some random scatter in the mean hole spacing.

Finally, the actual (nonlinear) breakup time,  $T_R$ , is compared with the predictions of the linear theory,  $T_L$ , in Figure 3 for  $B = 0$ ,  $B = 1$ , and  $B \gg 1$ . Nonlinearities accelerate the film breakup, since the destabilizing term,  $(H+B)H^2$ , grows stronger at locally thin spots, whereas stabilization due to surface tension,  $(H+B)H^2$ , becomes weaker as  $H \rightarrow 0$ . Interestingly, the ratio of nonlinear and linear breakup times is quite insensitive to the magnitude of the slip length,  $B$ . This is due to a compensation of nonlinear destabilizing and stabilizing effects in eq 12. For  $B \rightarrow 0$ , destabilizing and stabilizing terms scale as  $H^{-1}$  and  $H^3$ , respectively, at locally thin spots ( $H < 1$ ). For  $B \gg 1$ , destabilization is stronger ( $\propto H^{-2}$ ), but the stabilizing effect is also stronger ( $\propto H^2$ ). Thus, the actual breakup time is well represented by  $t_R = t_L f(\epsilon)$ , where  $f(\epsilon) < 1$  is the nonlinear ratio in Figure 3, which is largely independent of  $B$ , and  $t_L$  is given by eq 11.

The main conclusions from full nonlinear analysis are that while the length scale of instability leading to rupture is almost completely unaffected by slippage, the time scales for film breakup and subsequent dewetting can be greatly reduced. Indeed, the number density ( $\propto \lambda_m^{-2}$ ) of initial holes in polystyrene films ( $< 100$  nm) heated above their glass transition temperatures on silicon wafers is well predicted by eq 10,<sup>4,12</sup> which also holds for simple liquids without slip. In contrast,  $t_R$  for

nonslipping films ( $h_0 \sim 50$  nm,  $\mu \sim 100$  P,  $S \sim \gamma \sim 10$  mN/m,  $\varepsilon \sim 1$  nm) is about 4 days, whereas actual breakup and dewetting occur over time scales of minutes to hours.<sup>4-8</sup> Inclusion of slip ( $b \sim 10$   $\mu$ m) indeed reduces  $t_R$  to about 10 min. However, due to a very strong dependence of  $t_R$  on  $h_0$ , viz,  $t_R \propto h_0^6 \ln(h_0/\varepsilon)$ , slippage alone cannot explain the observed rapid rupture of relatively thick ( $>100$  nm) films (e.g., for  $h_0 = 100$  and 400 nm,  $t_R \sim 12$  h and 7 years, respectively!). For thick films, however, contaminants (e.g., dust particles) can play an important role in lowering the effective thickness to less than 100 nm, thereby engendering rapid breakup.<sup>6,7</sup>

Finally, suppression of slippage appears to be an important factor in *kinetic* stabilization of thin films.<sup>6-8</sup> One may anticipate suppression of slip when both of the following conditions are met: (a) strong end adsorption or grafting of a layer of long polymer chains on the surface and (b) significant interpenetration and entanglement of "free" chains with surface-bound immobile chains (polymer "brush"). At very low grafting density, suppression of slip should be minimal due to the paucity of anchoring sites. Interestingly, at very high grafting density also, slippage should again occur readily on the newly created interface between the "dry" brush and the free polymer on top. This is because the chain stretching at high density of packing engenders an entropic repulsion<sup>13,14</sup> which minimizes the interpenetration and entanglement coupling of free chains with the "brush" molecules. It would therefore appear that an intermediate density of grafting ("wet" brush) should be most effective (optimal) in kinetic stabilization by suppression of slip. Thermodynamically, exclusion of free polymer from the brush region also leads to "autophobicity" of melts on their own brushes, due to creation of a distinct nonwetable brush surface and a distinct brush-melt interface.<sup>8,13-15</sup> Thus, observed<sup>8</sup> stabilization (at low density of connector molecules) and dewetting (at high density) appear to have both kinetic (related to slippage) and thermodynamic (related to  $S$ ) reasons.

In another set of experiments,<sup>6,7</sup> films on a polymer brush were kinetically stabilized by adding long chains directly in the melt above their overlap concentration. Under these conditions, significant interpenetration and entanglement of free chains with the brush and each other are expected.<sup>7</sup> In addition to viscoelastic effects,<sup>7</sup> suppression of slip should also be an important factor in such systems.

The theory presented here should also aid the design of future experiments to assess the role of slippage in film rupture and help discriminate among the effects of slippage, contaminants, and viscoelasticity.

## References and Notes

- (1) Ruckenstein, E.; Jain, R. K. *J. Chem. Soc., Faraday Trans.* **1974**, *70*, 132.
- (2) Williams, M. B.; Davis, S. H. *J. Colloid Interface Sci.* **1982**, *90*, 2220.
- (3) Sharma, A.; Jameel, A. T. *J. Colloid Interface Sci.* **1993**, *161*, 190.
- (4) Reiter, G. *Phys. Rev. Lett.* **1992**, *68*, 75; *Langmuir* **1993**, *9*, 1344.
- (5) Redon, C.; Brzoska, J. B.; Brochard-Wyart, F. *Macromolecules* **1994**, *27*, 468.
- (6) Yerushalmi-Rozen, R.; Klein, J.; Fetters, L. *Science* **1994**, *263*, 793.
- (7) Yerushalmi-Rozen, R.; Klein, J. *Langmuir* **1995**, *11*, 2806.
- (8) Reiter, G.; Auroy, P.; Auvray, L. *Macromolecules* **1996**, *29*, 2150.
- (9) de Gennes, P.-G. *C. R. Acad. Sci.* **1979**, *228B*, 219.
- (10) Brochard, F.; Redon, C.; Sykes, C. *C. R. Acad. Sci.* **1992**, *314*, 19.
- (11) Sharma, A. *Langmuir* **1993**, *9*, 861.
- (12) Sharma, A.; Reiter, G. *J. Colloid Interface Sci.* **1996**, *178*, 383.
- (13) Leibler, L.; Ajdari, A.; Mourran, A.; Coulon, G.; Chatenay, D. In *Ordering in Macromolecular Systems*; Teramoto, A., Kobayashi, M., Norisuje, T., Eds.; Springer-Verlag: Berlin, 1994; pp 301-311.
- (14) Shull, K. *Faraday Discuss.* **1994**, *98*, 203.
- (15) Elizabeth, V.; Shull, K. R. *Macromolecules* **1995**, *28*, 6349.

MA9606162